

INTRODUCTION: 67455 is a very friable, feldspathic breccia that contains a variety of clast types, including pristine anorthosites. This rock was chipped from a large white boulder on the south rim of North Ray Crater together with 67475. Due to its friability it broke into several pieces during transport from the Moon (Fig. 1). Exact lunar orientation is unknown, but some exterior surfaces were recognized during the original processing by their discoloration and a few remaining zap pits. Much of the post-1974 work referenced here is the work of a consortium headed by Chao.



FIGURE 1. S-72-38194.

PETROLOGY: An extensive petrographic description is given by Minkin et al.(1977) and their terminology will be used here to avoid confusion. Several different clast types occur in a very friable groundmass of predominantly crushed and compacted plagioclase grains (Fig. 2). Monomineralic plagioclase dominates the clast population, with lesser amounts of olivine, pyroxene, metal, troilite, ilmenite, and lithic fragments. Metal grains in the groundmass tend to be rusty, with compositions outside of the “meteoritic” field (Fig. 3) (L.A. Taylor et al., 1973b). El Goresy et al. (1973a) report one occurrence of

sphalerite and “goethite” as a reaction rim around troilite. Lithic clasts include cataclastic anorthosites, gabbroic anorthosites, annealed feldspathic microbreccia and various glassy clasts. Modal abundances are summarized in Table 1 (reproduced from Minkin et al., 1977).

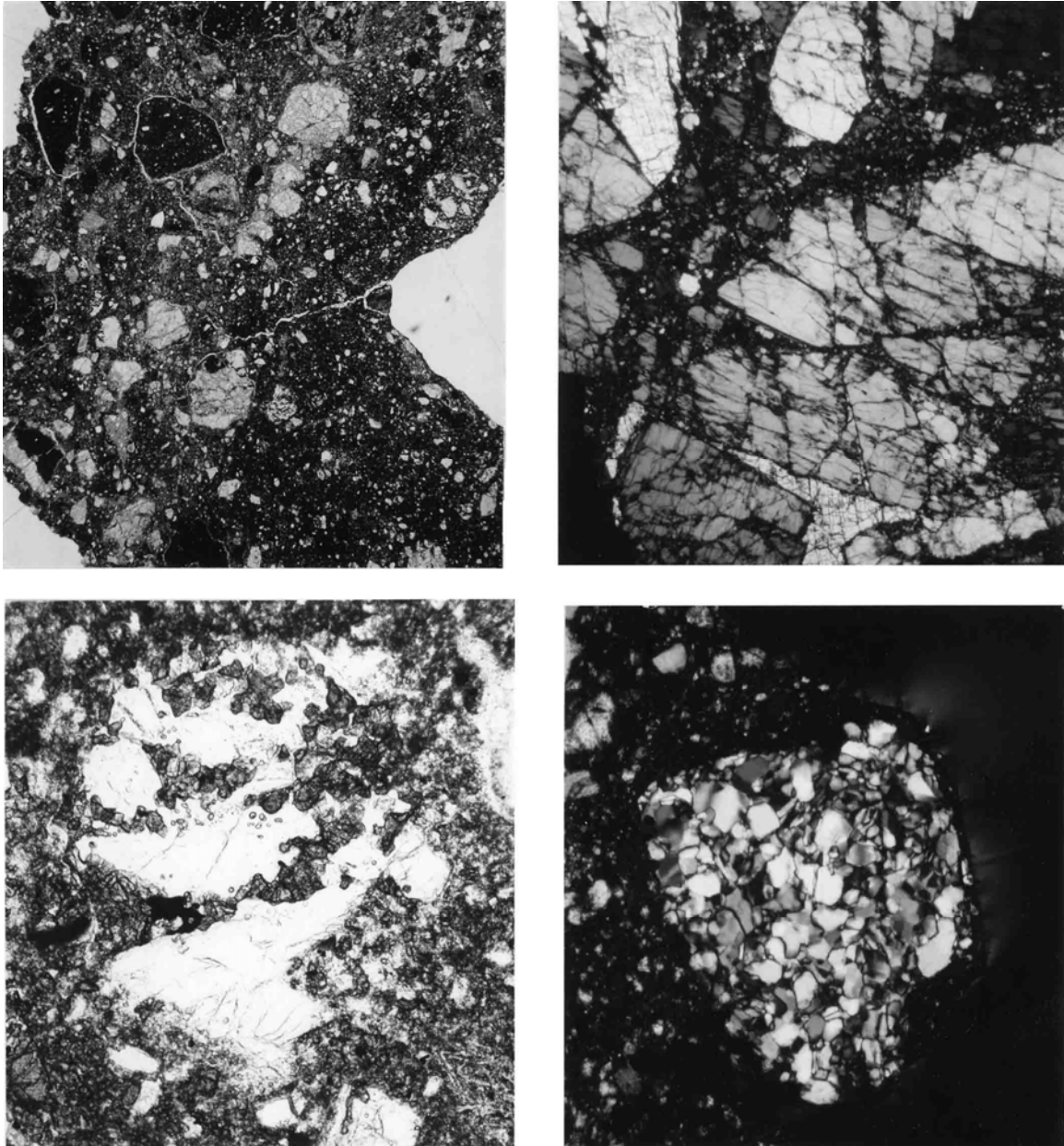


FIGURE 2.

- a) 67455,49. Whole thin section, ppl. Width about 10 mm.
- b) 67455,109. Shocked anorthosite clast, xpl. Width 2 mm.
- c) 67455,48. Gabbroic anorthosite clast, ppl. Width 1 mm.
- d) 67455,43. Feldspathic microbreccia clast, xpl. Width 1 mm.

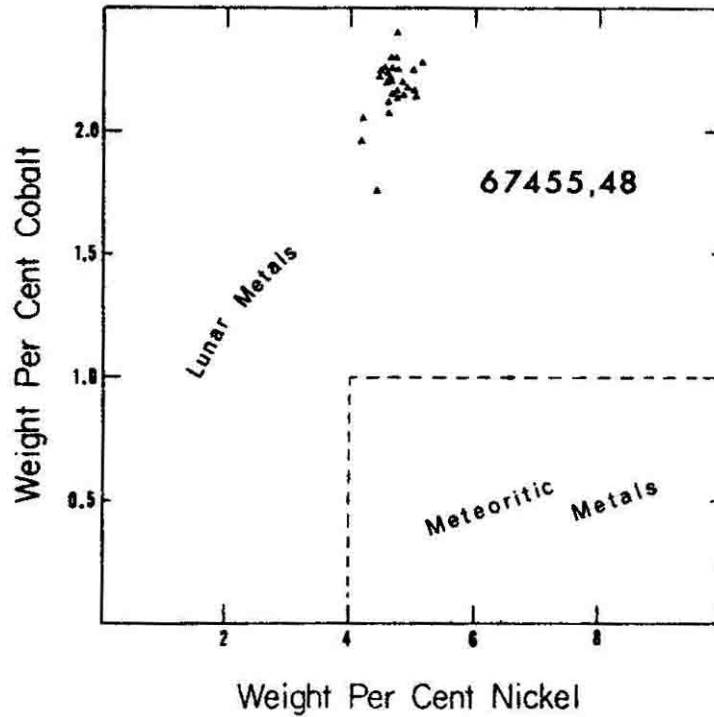


FIGURE 3. Metal compositions, from L. A. Taylor et al. (1973b).

TABLE 1. From Minkin et al. (1977).

Fragment population (> 40 μm) of 67455		
Fragment type	67455,50 (1554 counts)	67455,57 (825 counts)
Gabbroic anorthosite	7.9	9.1
Feldspathic microbreccia	2.7	6.8
Cataclastic anorthosite with olivine	0.7	3.4
Cataclastic anorthosite with pyroxene	5.0	3.4
Cataclastic anorthosite	8.3	4.4
Plagioclase	51.0	46.2
Olivine	3.7	6.2
Pyroxene	8.2	3.2
Glass:		
devitrified and brown with schlieren	0.5	0.9
annealed	0.8	0
coated grains	1.4	5.1
Fragment-laden melt:		
with plagioclase laths	3.4	2.5
without plagioclase laths	4.2	6.5
Opaque	2.2	2.3
Total	100.0	100.0

Weakly shocked, cataclastic anorthosite clasts often retain a cumulate texture (Fig. 2) with either olivine or pyroxene as interstitial phases. Not all cataclastic anorthosite clasts have interstitial mafics, but all contain elongate inclusions (generally $< 5 \mu\text{m}$) of olivine within the plagioclase crystals (Minkin et al., 1977). Mineral compositions in these clasts are typical of ferroan anorthosites (plagioclase An_{96-98} ; olivine Fo_{49-54} ; orthopyroxene $\text{Wo}_2\text{En}_{40}$, pigeonite $\text{Wo}_{5-7}\text{En}_{40-43}$; augite $\text{Wo}_{40-45}\text{En}_{35-30}$). Minor phases include interstitial ilmenite and troilite. Three cataclastic anorthosites were physically separated from the rock (,30, 31 and ,32), and found to be chemically pristine (see Ryder and Norman, 1978, for further descriptions and documentation of these particular clasts).

Gabbroic anorthosite clasts are largely recrystallized, though to varying degrees. Textures range from coarse granoblastic (Fig. 2) to very fine-grained “hornfelsic.” Pyroxene and olivine tend to occur in roughly equal amounts with interstitial ilmenite and metal. Mineral compositions are: plagioclase An_{92-97} , olivine Fo_{46-65} , pigeonite $\text{Wo}_{7-18}\text{En}_{54-48}$, augite $\text{Wo}_{20-40}\text{En}_{50-40}$ and orthopyroxene $\text{Wo}_{2-3}\text{En}_{63-56}$ (Minkin et al., 1977).

The feldspathic microbreccias of Minkin et al. (1977) consist entirely of many small ($< 30 \mu\text{m}$), anhedral plagioclase grains in a recrystallized mosaic (Fig. 2). These fragments could also be called “granoblastic anorthosite” or “recrystallized plagioclase.”

Two types of melt-glass clasts are recognized by Minkin et al. (1977): fragment-laden, glassy matrix breccia and xenocryst-free glasses. The glassy matrix breccia clasts tend to be very coherent, with abundant mineral and lithic fragments cemented by a small amount of interstitial melt. The interstitial melt is most often a dark brown glass, but in places shows a very faint poikilitic texture. Abundant xenocrysts and laths of plagioclase (An_{87-97} and An_{94-97} , respectively) and some olivine (Fo_{46-70}), orthopyroxene ($\text{Wo}_{2-3}\text{En}_{58-77}$), augite ($\text{Wo}_{31-43}\text{En}_{41-38}$) and lithic fragments are all found within the glassy matrix clasts. Xenocryst-free glasses, most of which possess schlieren, are uncommon. Some are strained as indicated by their wavy extinction, while others show evidence of annealing or devitrification. The lack of glass spherules in the rock indicates that no significant regolith component is present (Minkin et al., 1977).

CHEMISTRY: Lindstrom et al. (1977) and Hertogen et al. (1977) provide major element, lithophile, siderophile and volatile element data on a suite of separated clast and matrix samples. Reed et al. (1977) and Jovanovic and Reed (1978) provide data on volatile metals, halogens, and other trace elements for some of these same samples. Other major and trace element analyses of the bulk rock are given by Rose et al. (1973), Wanke et al. (1973,1977), Fruchter et al. (1974) and Muller (1975). (The analysis listed as 67455,13 in Fruchter et al., 1974, is actually of 68115,78). Bulk C, N and S data are reported by Moore et al. (1973), Cripe and Moore (1974) and Moore and Lewis (1976). Wrigley (1973) provides natural and cosmogenic radionuclide abundances. Defocused-beam microprobe analyses of several clast types are given by Minkin et al. (1977).

All of the bulk analyses show 67455 to be a highly aluminous breccia with relatively low levels of both lithophiles and siderophiles and a somewhat high Fe/Mg (Table 2, Figs. 4, 5, 6, and 7). The very low C and N abundances (Table 2) indicate a negligible solar wind component in the bulk breccia.

The major and lithophile element compositions of the clast population can be accounted for by mixing a relatively ferromagnesian, REE-rich component with an aluminous, REE-poor component (Figs. 4, 5, and 6) (Lindstrom et al., 1977). These two end-members are represented petrographically by the glassy matrix breccia or some of the recrystallized breccia clasts, and the cataclastic ferroan anorthosite clasts, some of which are pristine. The bulk matrix is, however, somewhat enriched in REEs relative to those two components (Figs. 6 and 7) and a third component seems to be required. To match the petrographically observed abundances of clasts, which require ~70-80% anorthositic material (Table 1), Lindstrom et al. (1977) postulate a “gabbroic anorthosite” component with 28-30% Al_2O_3 REEs ~10 X chondrites as this cryptic third end-member.

All of the clasts and matrix samples analyzed by Hertogen et al. (1977) have low abundances of meteoritic siderophiles (Table 2). Three of the cataclastic anorthosite clasts have low enough levels of these elements to be classified as chemically pristine. Only meteoritic groups 5H and 7, groups common in rocks from North Ray Crater, are recognized in tile 67455 samples (Hertogen et al., 1977).

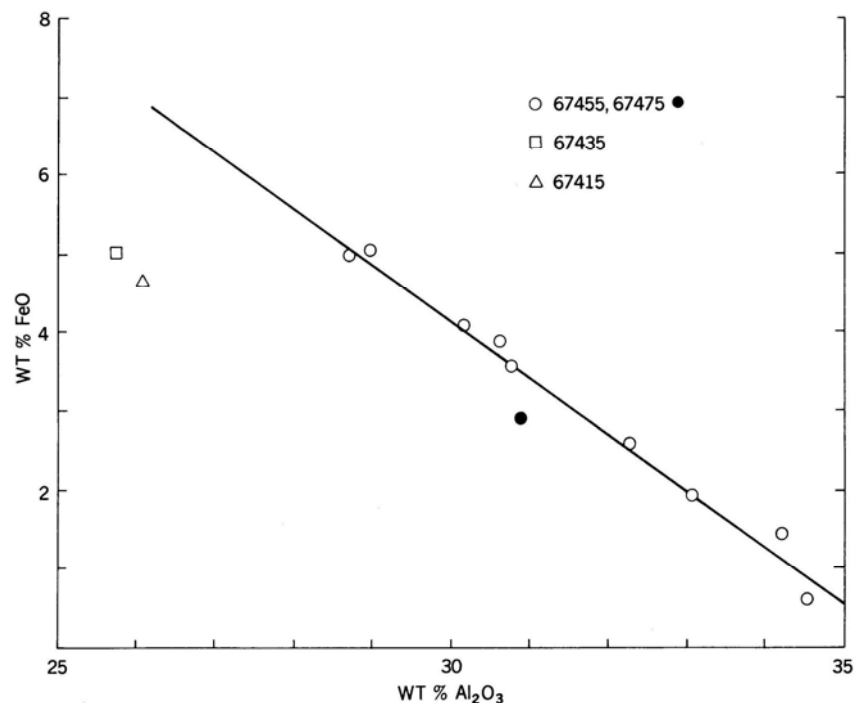


FIGURE 4. Variation of FeO with Al_2O_3 for clast and matrix samples of 67455, and bulk samples of 67415, 67435, and 67475; from Lindstrom et al. (1977). The lines in Figures 4 and 5 represent linear regressions on the 67455 and 67475 data.

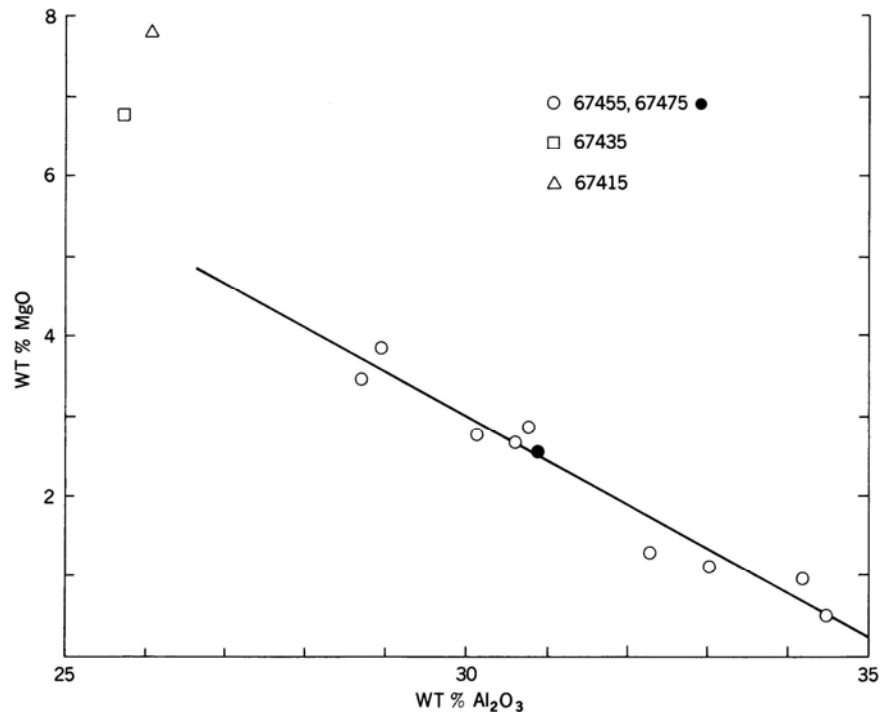


FIGURE 5. Variation of MgO with Al₂O₃ for clast and matrix samples of 67455, and bulk samples of 67415, 67435, and 67475. From Lindstrom et al. (1977).

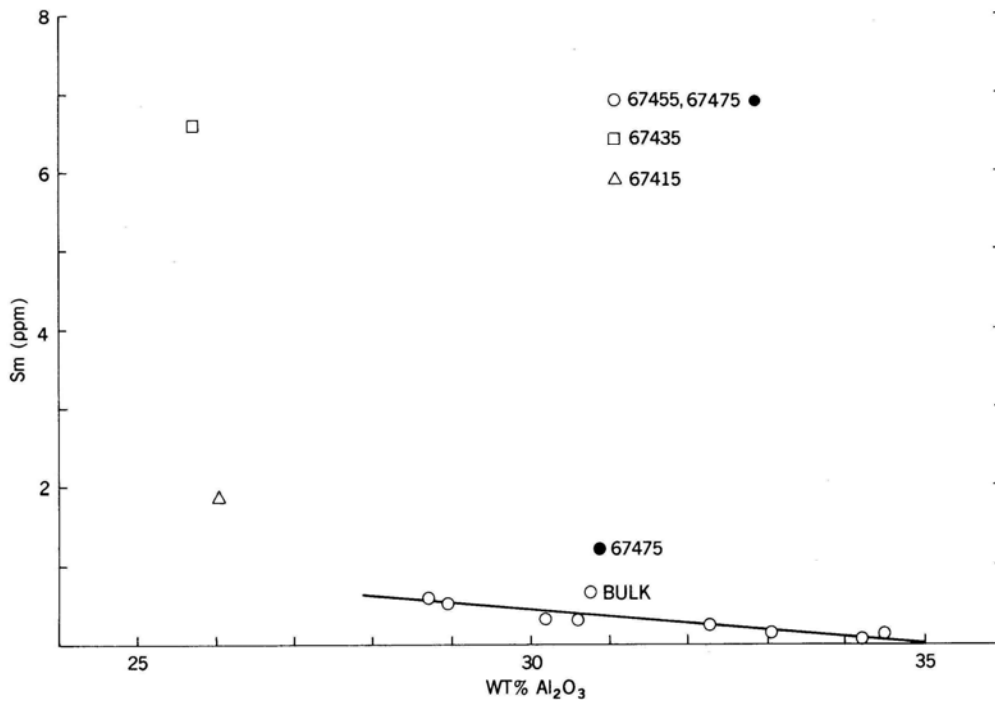


FIGURE 6. Variation of Sm with content for samples from the White Breccia Boulders. The line is a linear regression for 67455 clast data. From Lindstrom et al. (1977).

TABLE 2. Summary chemistry of 67455 lithologies.

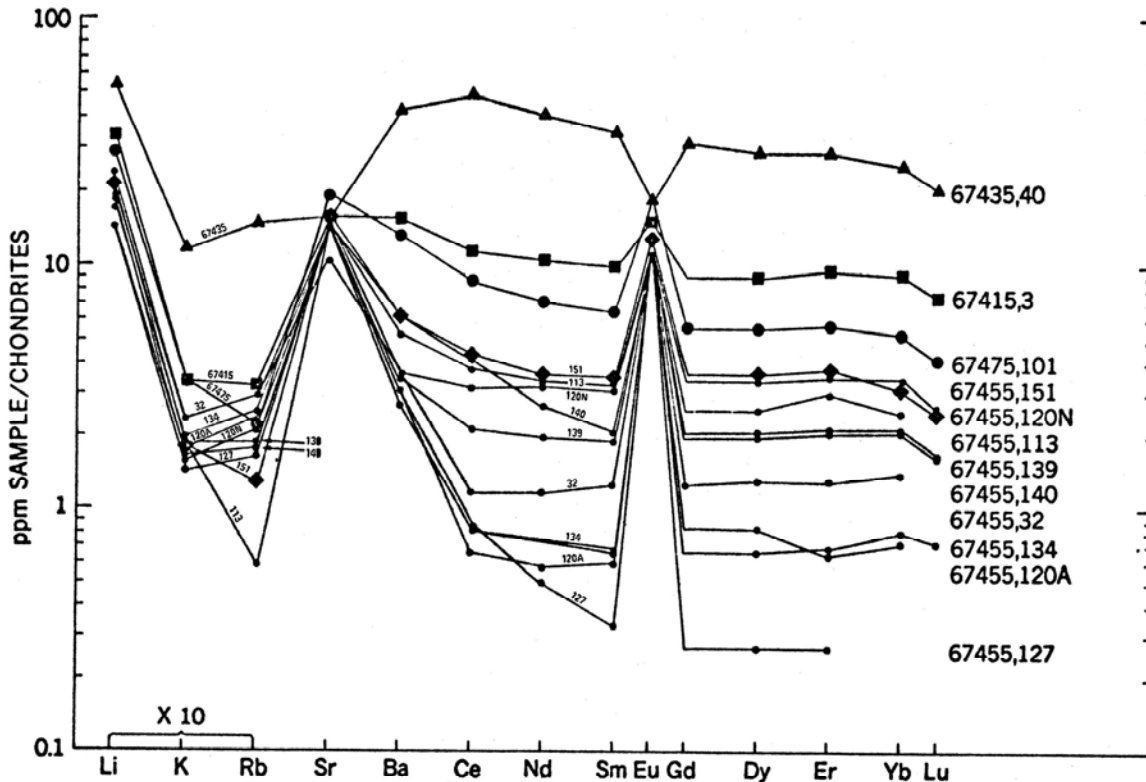
	<u>Bulk rock</u>	<u>Cataclastic anorthosite clasts, pristine</u>	<u>Glassy matrix breccia clasts</u>
SiO ₂	44.8	44.7	44.4
TiO ₂	0.25	<0.1	0.23
Al ₂ O ₃	31.1	33.2	28.7
Cr ₂ O ₃	0.07	<0.01	0.05
FeO	4.0	2.0	5.0
MnO	0.05	0.018	0.07
MgO	3.0	1.1	3.5
CaO	17.8	18.4	17.0
Na ₂ O	0.37	0.39	0.47
K ₂ O	0.024	0.023	0.023
P ₂ O ₅	0.02	~0.02	0.02
Sr	150	145	152
La	1.1	~0.3	~1
Lu	0.09	~0.025	0.089
Rb	0.6	0.7	0.17
Sc	7.7		
Ni	26	<7	7.9
Co	8		
Ir ppb	1.08	0.003	1.23
Au ppb	0.355	0.008	0.12
C	8		
N	10		
S	<20		
Zn	7.5	~3	4.13
Cu	1.9		

Oxides in wt%; others in ppm except as noted.

RADIOGENIC ISOTOPES/GEOCHRONOLOGY: Schaeffer and Schaeffer (1977) report Ar isotopic data for the bulk rock. A gas-release plateau could not be obtained. ⁴⁰Ar has apparently been lost through diffusive processes and the >1200°C fractions show evidence for excess ³⁸Ar.

Kirsten et al. (1973) give Ar data for two clasts, one dark and one light, separated by them from a bulk sample. The dark clast failed to yield a plateau while the light clast gave a plateau age of 3.91 ± 0.12 b.y.

Assuming that the total K-Ar age gives a lower limit to the age of the rock (e.g. Turner and Cadogan, 1975) and that the rock is younger than the clasts it contains, 67455 is thus bracketed to be between 3.80-4.03 b.y. old.



Lithophile trace element abundances for samples from the White Breccia Boulders. The light REE analyses for 67455,140 and 67455,127 are not reliable because of large blank and spike corrections on very small anorthositic samples.

FIGURE 7. Rare earths for clast and matrix samples, from Lindstrom et al. (1977).

RARE GASES/EXPOSURE AGES/TRACKS: Published exposure ages are given in Table 3. These ages place the age of North Ray Crater at ~40-50 m.y. Kr and Xe isotopic data are reported by Drozd et al. (1974), Drozd (1974), and Bernatowicz et al. (1978) (Figs. 8 and 9). The unusual low temperature release peak of Xe (Fig.10) is ascribed to lightly bound, surficial gas by Bernatowicz et al. (1978). Drozd (1974) and Bernatowicz et al. (1978) disagree on whether or not excess fission Xe is present in 67455. The latter authors suggest the possibility of a variation in the trapped gas component.

TABLE 3. Exposure ages of 67455.

<u>Method</u>	<u>Age (m.y.)</u>	<u>Reference</u>
⁸¹ Kr-Kr	50.2 _{-1.8}	Drozd <u>et al.</u> (1974)
²¹ Ne	17.3 _{-4.1}	"
³⁸ Ar	38.0 ₊₁₃	"
³⁸ Ar (dark clast)	31 ₋₂	Kirsten <u>et al.</u> (1973)
³⁸ Ar (light clast)	33 ₋₂	"
³⁸ Ar	35	Schaeffer and Schaeffer (1977)
Cosmic ray tracks	~30	Storzer <u>et al.</u> (1973)

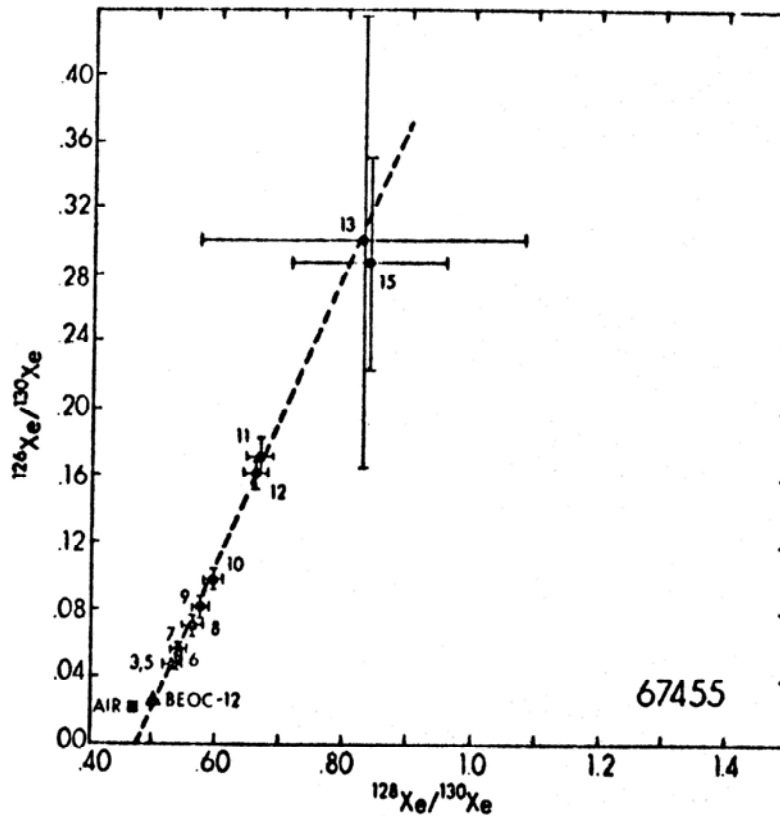


FIGURE 8. From Bernatowicz et al. (1978).

Pepin et al. (1974) note that total ^{21}Ne and ^{38}Ar ages are usually significantly lower than the ^{81}Kr -Kr ages, and calculate the shielding depth within the rock necessary to account for these lower ages. For three North Ray Crater rocks, these depths range from ~ 3 - 6 g/cm^2 . The data are consistent with the ejection of the 67455 boulder from a well-shielded location with no significant pre-surface irradiation history to its present location in a single event (Drozd et al. 1974; Pepin et al., 1974).

^{26}Al and ^{22}Na are given by Wrigley (1973). 67455 is probably not saturated in ^{26}Al activity (Yokoyama et al., 1974).

Cosmic ray tracks in 67455 feldspars indicate a trace of ancient solar flare irradiation prior to breccia formation (Storzer et al., 1973).

PHYSICAL PROPERTIES: Basic magnetic and natural remanent magnetization characteristics of a bulk rock split are given by Nagata et al. (1973,1975). 67455 is an example of a rock whose dependence of coercive force (H_c) and saturation remanence (I_R) on temperature is characterized by an asymmetrical distribution around a low temperature spike (Fig. 11). Such a peak may represent the blocking temperature of a population of fine metallic grains (Nagata et al., 1973).

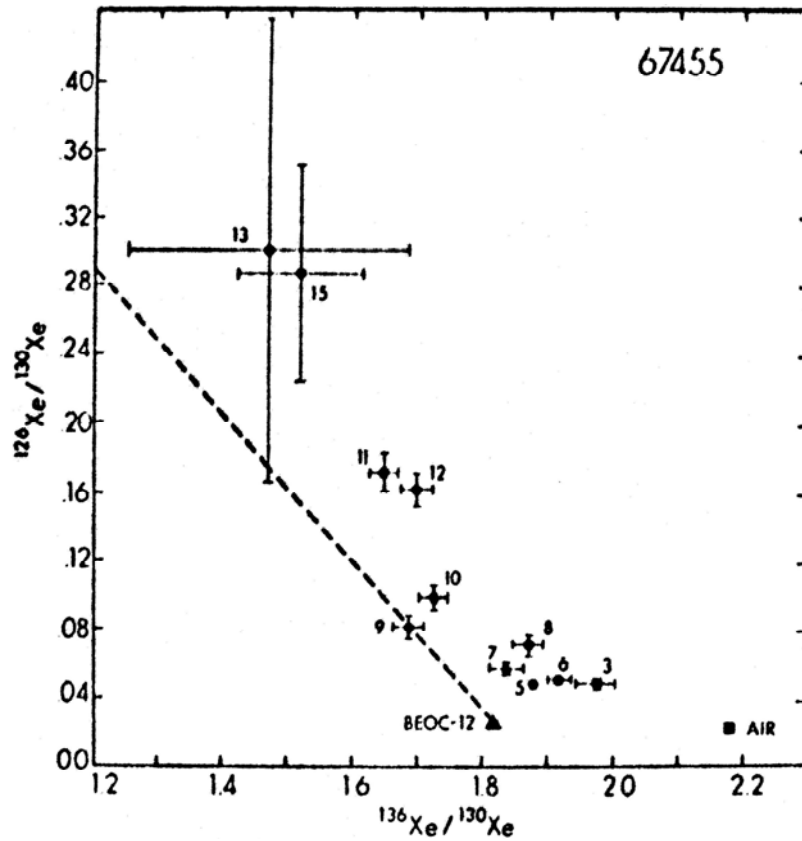


FIGURE 9. From Bernatowicz et al. (1978).

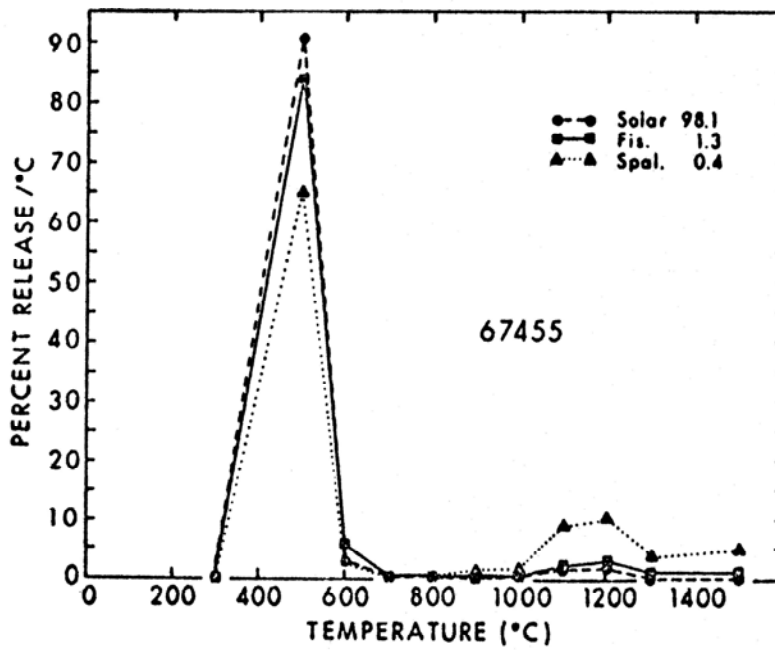
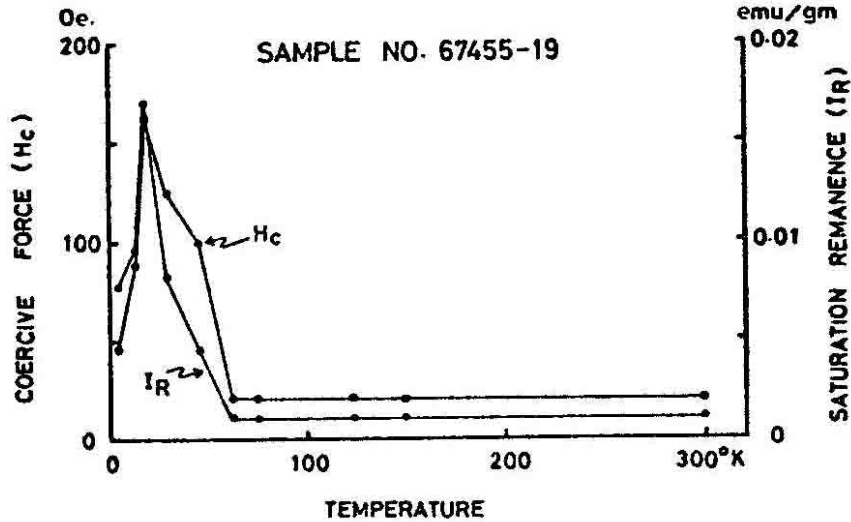


FIGURE 10. Xe isotopic data. From Bernatowicz et al. (1978).



Example of Group III of the dependence of H_c and I_R on temperature; there is a sharp increase in H_c and I_R at a critical temperature (T^*) and the largest value of H_c at the low temperature is reasonably close to $\frac{1}{2}H_{RC}$.

FIGURE 11. Magnetic parameters, from Nagata et al. (1973).

Schwerer et al. (1973) and Huffman et al. (1974) tabulate the distribution of Fe among the mineral phases and the Fe^0/Fe^{2+} ratio of 67455 as determined by Mossbauer and magnetic techniques. Very little Fe-metal (~ 0.02 wt%, 2.5% Ni) is present in this-rock (see also Nagata et al., 1973).

IR and UV spectral reflectance and other polarimetric property measurements are given by Adams and McCord (1973), Dollfus and Geake (1975), Hua et al. (1976) and Zellner et al. (1977) (Figs. 12 and 13).

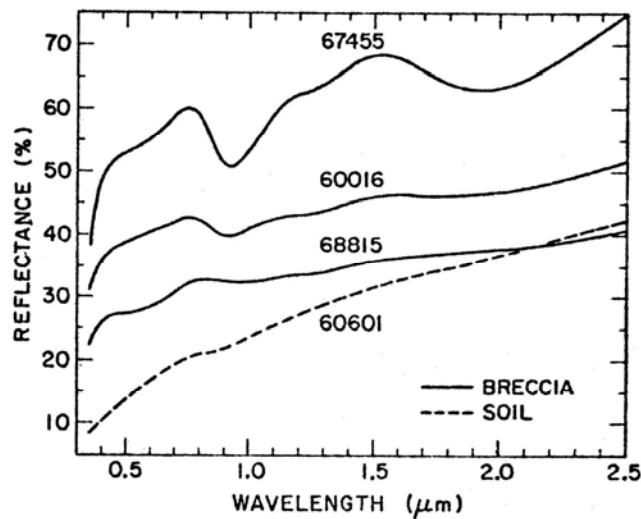
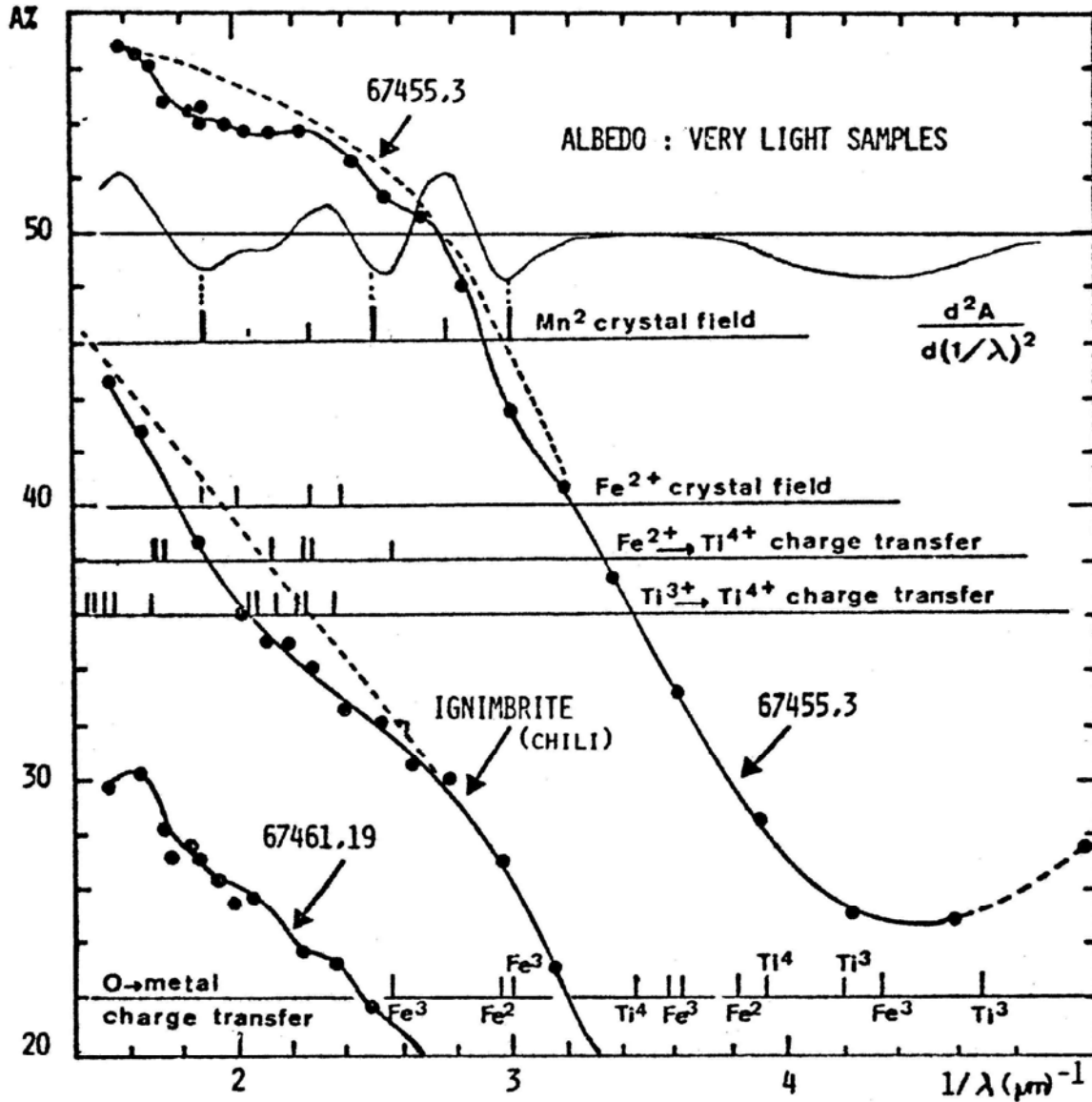


FIGURE 12. Spectral reflectance curves, from Adams and McCord (1973).

Weeks (1973b) reports electron paramagnetic resonance (EPR) spectral data. Huffman and Dunmyre (1975) studied superparamagnetic Fe^{2+} spin clusters in olivine. 78% of the Fe^{2+} 67455 olivines are contained within such clusters.



Spectral diffuse reflectance curves for very light samples. Second-derivative curve for lunar sample 67455,3 enhancing the absorption features.

FIGURE 13. Spectral reflectance curves, from Hua et al. (1976).

PROCESSING AND SUBDIVISIONS: 67455 was removed from its documented bag in several pieces. In 1972, during the original round of allocations, individual fragments and chips from one of the larger pieces were assigned split numbers (Fig. 14). In 1974, under the direction of Chao, the powder residue was passed through a 2 mm sieve to recover clasts and fragments. Chao then classified these >2 mm fragments (total weight 47.1 g) macroscopically into 6 groups and assigned each group a split number (,35 - ,40). Individual fragments representative of each group were selected by Chao for allocation to members of his consortium.

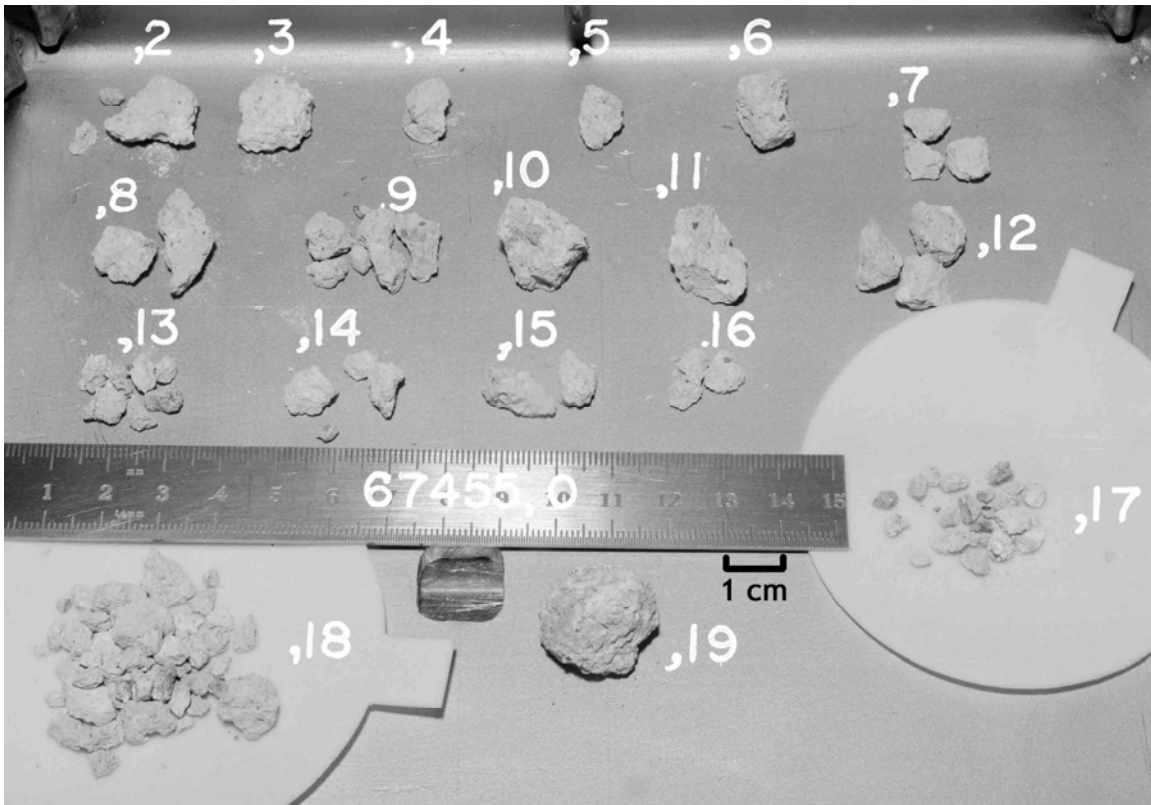


FIGURE 14. S-72-51830.